IOP Publishing Environ. Res. Lett. 16 (2021) 094005 https://doi.org/10.1088/1748-9326/ac1818

ENVIRONMENTAL RESEARCH
LETTERS

CrossMark

OPEN ACCESS

RECEIVED
24 May 2021

REVISED
21 July 2021

ACCEPTED FOR PUBLICATION
27 July 2021

PUBLISHED
12 August 2021

LETTER

The role of enhanced rock weathering deployment with agriculture in limiting future warming and protecting coral reefs

Negar Vakilifard[1], **Euripides P Kantzas**[2], **Neil R Edwards**[1,3], **Philip B Holden**[1] and **David J Beerling**[2]

[1] Environment, Earth and Ecosystems, The Open University, Milton Keynes, United Kingdom
[2] Leverhulme Centre for Climate Change Mitigation, Department of Animal and Plant Sciences, University of Sheffield, Sheffield, United Kingdom
[3] Cambridge Centre for Environment, Energy and Natural Resource Governance, University of Cambridge, Cambridge, United Kingdom

E-mail: negar.vakilifard@open.ac.uk

Keywords: coral reefs, enhanced rock weathering, Earth system model, ocean acidification, Paris agreement temperature targets, RCP2.6

Supplementary material for this article is available online

Abstract

Meeting the net-zero carbon emissions commitments of major economies by mid-century requires large-scale deployment of negative emission technologies (NETs). Terrestrial enhanced rock weathering on croplands (ERW) is a NET with co-benefits for agriculture, soils and ocean acidification that creates opportunities for generating income unaffected by diminishing carbon taxes as emissions approach net-zero. Here we show that ERW deployment with croplands to deliver net 2 Gt CO_2 yr^{-1} removal approximately doubles the probability of meeting the Paris 1.5 °C target at 2100 from 23% to 42% in a high mitigation Representative Concentration Pathway 2.6 baseline climate. Carbon removal via carbon capture and storage (CCS) at the same rate had an equivalent effect. Co-deployment of ERW and CCS tripled the chances of meeting a 1.5 °C target (from 23% to 67%), and may be sufficient to reverse about one third of the surface ocean acidification effect caused by increases in atmospheric CO_2 over the past 200 years. ERW increased the percentage of coral reefs above an aragonite saturation threshold of 3.5 from 16% to 39% at 2100, higher than CCS, highlighting a co-benefit for marine calcifying ecosystems. However, the degree of ocean state recovery in our simulations is highly uncertain and ERW deployment cannot substitute for near-term rapid CO_2 emissions reductions.

1. Introduction

A rapid transition to a low-carbon economy is essential to avoid breaching the Paris Agreement climate targets. However, this transition is insufficient to meet the mid-century net-zero carbon emission commitments of major economies, including the UK, EU, China and Japan, without large-scale deployment of negative emission technologies (NETs) (Hartmann *et al* 2013, Board and Council 2015). It is generally assumed that NET deployment will be funded by redistribution of income from local or global carbon taxation (Honegger and Reiner 2018, Bednar *et al* 2019), but this income source will diminish as emissions, and resulting carbon-tax receipts, reduce with the transition to clean energy advances. Hence, the deployment of NETs with co-benefits impacting multiple economic sectors could provide valuable opportunities to incentivise continued active carbon drawdown. Such efforts might then allow existing regulation and incentive schemes to be re-purposed and strengthened to encourage carbon sequestration without direct reliance on carbon pricing (Cox and Edwards 2019). Furthermore, the re-purposing of existing policy frameworks may facilitate an earlier introduction of negative emissions, potentially another critical enabling factor in the ultimate achievement of ambitious mitigation targets.

Terrestrial enhanced rock weathering (ERW) is a NET removing atmospheric CO_2 by accelerating natural chemical breakdown of silicate rocks, ultimately locking the carbon in ocean, sediments and soils. ERW releases base cations (primarily Ca^{2+} and Mg^{2+}) and delivers alkalinity (HCO_3^- and CO_3^{2-}) via runoff to the river systems and ultimately to the ocean. The residence time of these anions in the global ocean is on the order of 100000–1000000 years, making it a permanent carbon storage reservoir on human timescales (Renforth and Henderson 2017, Beerling *et al* 2018). In soil, the precipitation of secondary carbonate minerals from the release of base cations can create another sink for CO_2, if soil pore water is supersaturated with respect to carbonate minerals (Manning and Renforth 2013). ERW may have utility in decarbonisation scenarios required for net-zero because of its potential co-benefits for agriculture and marine sectors, including crop yield enhancement and mitigation of both terrestrial N_2O emissions and ocean acidification (Köhler *et al* 2010, Hartmann *et al* 2013, Taylor *et al* 2016, Beerling *et al* 2018, Kelland *et al* 2020).

Here, we evaluate the effects of an optimised, multi-national strategy designed to achieve a net carbon dioxide removal (CDR) goal of 2 Gt CO_2 yr^{-1} via ERW deployment with croplands (Beerling *et al* 2020) using an intermediate complexity Earth system model, the grid-enabled integrated Earth system model (GENIE) (Holden *et al* 2013a). The net CDR goal of 2 Gt CO_2 yr^{-1} accounts for secondary CO_2 emissions from logistical ERW supply chain operations (mining, grinding, transporting and spreading) and constraints on energy availability for rock grinding (Beerling *et al* 2020). It is lower than earlier detailed theoretical assessments of the effect of widespread ERW application on tropical ecosystems, which neglected practical constraints related to energy cost, safety and conservation (Taylor *et al* 2016, Strefler *et al* 2018).

Building on prior Earth system assessments of tropical forest ERW deployment (Köhler *et al* 2010, 2013, Taylor *et al* 2016), we focus on global atmospheric CO_2, climate and ocean biogeochemistry feedbacks of cropland ERW over the coming century. Our analysis considers undertaking ERW practices in the context of the Intergovernmental Panel on Climate Change's (IPCC) high mitigation scenario, Representative Concentration Pathway (RCP) 2.6 (van Vuuren *et al* 2011). Assessing ERW effectiveness with RCP2.6 allows examination of the effects of additional NET deployment within a scenario that assumes existing international cooperation for mitigating CO_2 through climate policies. Furthermore, we compared Earth system responses to ERW with carbon capture and storage (CCS) NET of an equivalent annual CO_2 drawdown, and co-deployment of ERW and CCS strategies to examine potential interactions on CDR efficacy.

Biogeochemical feedbacks assessed include changes in CO_2 concentration, mean global warming, surface ocean pH and ocean aragonite saturation state, a key variable affecting coral reef health (Mollica *et al* 2018). To quantify uncertainty, we used an 86-member ensemble with GENIE, pre-calibrated to satisfy large-scale constraints on the preindustrial state (Holden *et al* 2013b) and historical transient warming and carbon sinks (Holden *et al* 2013a, Foley *et al* 2016).

2. Methods

2.1. GENIE model simulations

We developed three GENIE simulation experiments adopting a high mitigation baseline (RCP2.6, the postscript 2.6 denoting radiative forcing in Wm^{-2} in year 2100 relative to year 1750): (a) ERW with 2 Gt CO_2 yr^{-1} removal, (b) CCS with 2 Gt CO_2 yr^{-1} removal, (c) co-deployment of ERW with CCS giving a total of 4 Gt CO_2 yr^{-1} removal. GENIE version 2.7.7 (Holden *et al* 2013a, 2013b) consists of seven main modules for studying Earth system dynamics and making long-term future predictions. The physical model is the combination of a 3D frictional geostrophic ocean model (GOLDSTEIN) (at 36 × 36 grid-cells horizontal resolution with 16 vertical levels), a 2D energy moisture balance model of the atmosphere and a thermodynamic/dynamic sea–ice model. The land surface carbon storage is modelled with the efficient numerical terrestrial scheme. The rock-weathering module ROKGEM (Colbourn *et al* 2013) is included to redistribute prescribed weathering fluxes according to a fixed river-routing scheme. The potentially beneficial effect of ERW on marine ecosystems via enhanced nutrient fluxes from terrestrial to ocean components was not considered in the analysis.

The ocean biochemistry model (BIOGEM) (Ridgwell *et al* 2007) includes cycling of iron based on Annan and Hargreaves (2010) for estimation of the changes in phosphate and dissolved organic phosphorous concentrations. The deep-sea sediment module (SEDGEM) (at a 36 × 36 resolution) is based on the cycling of carbon and alkalinity together with the essential nutrients, phosphate, silicic acid and iron (Ridgwell 2001, Ridgwell and Hargreaves 2007).

For each model experiment, GENIE was run for an ensemble of 86 different parameter sets to capture a wide range of possible climate responses. Each ensemble member employs a different combination of 28 parameters filtered from a wide range of plausible input values. The filtering process uses emulation of input parameter space to produce reasonable preindustrial climates (Holden *et al* 2013a) and through transient simulations with historical forcing from AD 850 including land use change to give plausible climate-change responses (Holden *et al* 2013b, Foley *et al* 2016). The future NET scenarios (beginning at 2020) were based on RCP2.6 GENIE settings (Zickfeld *et al* 2013) for the period of 80 years till the end of the century. The carbon cycle effects of ERW and CCS are both modelled as a reduction in anthropogenic CO_2 emissions. In the case of ERW, approximately 2/3 of this carbon is returned to the system through a bicarbonate flux to the ocean with the remainder, representing pedogenic carbon, removed

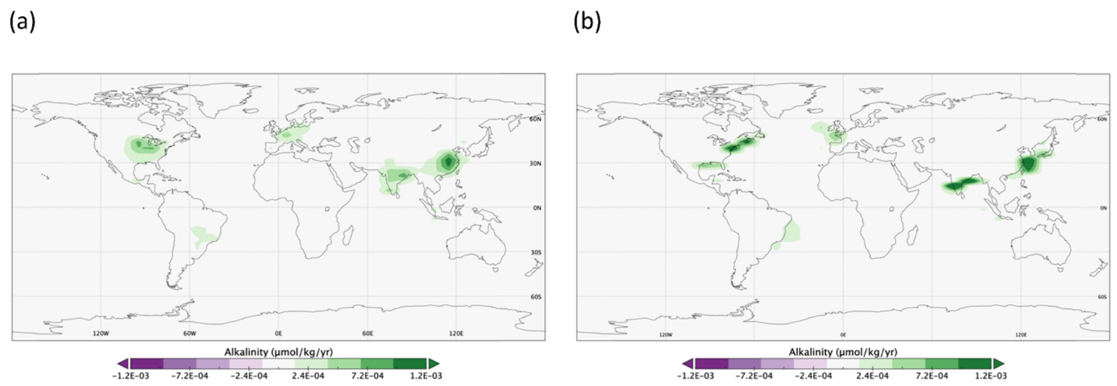

Figure 1. Average annual alkalinity fluxes from croplands calculated with a global model of ERW (Beerling *et al* 2020) re-gridded to the GENIE (an Earth system model) grid resolution: (a) on land and (b) at the point of entering the ocean.

permanently (see following section 2.2 for details). For each NET scenario, the likelihood of meeting the Paris agreement temperature targets was estimated as the percentage of the ensemble members with peak and 2100 warming below the relevant thresholds.

2.2. Alkalinity flux data

The impact of ERW-induced alkalinity fluxes on the Earth system was investigated by introducing decadal average bicarbonate fluxes calculated with a global ERW model based on a model of rock weathering within the soil profile (Beerling *et al* 2020) as an input to GENIE. The ERW model uses an optimisation procedure accounting for environmental conditions, available energy for rock dust grinding and transportation costs to determine regions most suitable for ERW on a nation-by-nation basis. We assumed a 2:1 partitioning of a global net 2 Gt CO_2 yr^{-1} CDR between an alkalinity flux of 1.3 Gt CO_2 yr^{-1} delivered into the oceans and 0.7 Gt CO_2 yr^{-1} sequestered via soil carbonate formation, as determined by the ERW modelling (Beerling *et al* 2020). Average annual alkalinity fluxes were re-gridded to the GENIE grid resolution ($10^\circ \times (3\text{–}19)^\circ$ equal area cells) (figure 1(a)) and runoff from coastal cells to the ocean determined by the runoff scheme in GENIE (Edwards and Marsh 2005) (figure 1(b)).

This idealized analysis assumes a constant ERW derived alkalinity flux for 2020–2100, and the same procedure is used in the ERW and CCS co-deployment simulations. A preliminary estimation of the significance of the effect of climate change on CDR with ERW was conducted offline using the GENIE natural weathering module ROKGEM (Colbourn *et al* 2013). The module was first forced with ensemble averaged fields of surface air temperature:

$$F_{\mathrm{CaSiO_3}} = F_{\mathrm{CaSiO_3},0}\,\mathrm{e}^{-\frac{E_a}{R}\left(\frac{1}{T}-\frac{1}{T_0}\right)} \quad (1)$$

where $F_{\mathrm{CaSiO_3}}$ is the alkalinity flux (mol yr^{-1}), E_a is the activation energy for dissolution (63 kJ mol^{-1}) (Brady 1991), T is spatial temperature (K) and R is the molar gas constant (8.31 J K^{-1} mol^{-1}) (Colbourn *et al* 2013). The index zero stands for the initial value.

The alkalinity flux was then modified ($F_{\mathrm{CaSiO_3,m}}$) to include the terrestrial gross primary productivity and runoff feedbacks under RCP2.6:

$$F_{\mathrm{CaSiO_3,m}} = F_{\mathrm{CaSiO_3}}\left(\frac{P}{P_0}\right)\left(1+k_{\mathrm{run}}\left(T_g - T_{g,0}\right)\right)^{\beta} \quad (2)$$

where P is the spatial productivity (kgC m^{-2} yr^{-1}), T_g is the global temperature (K) and k_{run} (K^{-1}) and β are global runoff constants set to 0.25 (New *et al* 1999, Fekete *et al* 2000, 2002) and 0.8 (West *et al* 2005), respectively. The index zero denotes the initial value.

2.3. ERW mitigation of agricultural N_2O

In GENIE, a globally uniform perturbation to the radiative forcing is applied to account for unmodelled forcing agents such as non-CO_2 trace gases. The climatic effect of reduced agricultural N_2O emissions resulting from ERW practices uses this approach, deriving the radiative forcing in a two-stage process. We first estimate agricultural N_2O emissions by projecting 2010–2030 estimates (Reay *et al* 2012) and assume a 40% reduction from these (Blanc-Betes *et al* 2021), resulting in around 4.4 Tg N_2O yr^{-1} emissions reduction from 20% of the global cropland regions treated with ERW. The total cropland area of 2.96 Mkm^2 was estimated based on the net 2 Gt CO_2 yr^{-1} CDR scenario in (Beerling *et al* 2020) which considers ERW deployment on the percentage of agricultural lands of China (55%), USA (55%), India (51%), Brazil (51%), Indonesia (59%), Canada (35%), Mexico (52%) and the European nations, France (54%), Germany (57%), Italy (55%), Spain (41%) and Poland (38%). We recognize that reductions in N_2O with ERW treatment using basalt need evaluation across a wider range of crop and soil types, and climates, but developed this model experiment as a first test to estimate an upper bound of ERW N_2O mitigation effects on climate. The estimated N_2O emission reductions are then converted to equivalent CO_2 (based on the greenhouse gas global warming potential over 100 years (GWP-100) (IPCC 2001)) and subtracted from global CO_2 emissions through time in a sensitivity experiment. A radiative forcing time series was then diagnosed from the perturbed CO_2 concentration using (IPCC 2001):

$$\Delta F(t) = \alpha \ln \left(\frac{C^N(t)}{C(t)} \right) \quad (3)$$

where $\Delta F(t)$ is the radiative forcing due to CO_2 concentration (Wm^{-2}) at time t, α is a constant equal to 5.35 Wm^{-2}, $C^N(t)$ is the atmospheric CO_2 concentration (ppm) in the N_2O forced experiment, $C(t)$ atmospheric CO_2 concentration (ppm) in the baseline. The non-CO_2 trace gas radiative forcing was adjusted by $\Delta F(t)$ in the ERW and co-deployment simulations.

2.4. Sensitivity of the coral reefs to the ocean acidification

We investigated the ocean biogeochemical implications of each scenario (ERW, CCS, and ERW with CCS) for coral reef oceanic environments by calculating changes in pH and the aragonite saturation state (Ω_{arg}) of surrounding waters derived from GENIE simulations. Saturation state Ω_{arg} is defined as (Zeebe and Wolf-Gladrow 2001, Ridgwell *et al* 2007, Gattuso and Hansson 2011):

$$\Omega_{arg} = \frac{\left[Ca^{2+}\right]\left[CO_3^{2-}\right]}{K_{sp}}. \quad (4)$$

Where $\left[Ca^{2+}\right]$ and $\left[CO_3^{2-}\right]$ are the concentrations of calcium and carbonate ions in terms of mol kg^{-1}, respectively. K_{sp} is a solubility constant $mol^2\ kg^{-2}$ calculated from the empirical formula in (Millero 1995) and varies with temperature and salinity. We used three different Ω_{arg} thresholds (3, 3.25 and 3.5) for each scenario, given that the critical threshold varies across different coral populations (Kleypas 1999, Guinotte *et al* 2003, Ricke *et al* 2013). Reef locations were extracted from Reef Base Global Database (Tupper *et al* 2011) (supplementary material figure S1 (available online at stacks.iop.org/ERL/16/094005/mmedia)) and the data re-gridded to GENIE grid resolution. For each grid cell containing reefs, the associated Ω_{arg} value was assigned and compared with the defined critical aragonite saturation to determine the percentage of reef locations surrounded by supersaturated waters.

3. Results

3.1. NETs help achieve the 1.5 °C Paris agreement target

According to our Earth system simulations, application of either NET (ERW or CCS) slowed the atmospheric CO_2 growth rate and lowered peak atmospheric CO_2 concentrations by ~6 ppm at 2050 and 11 ppm at 2100 (figure 2(a)). These results are approximately a quarter of the end-of-century atmospheric CO_2 reduction by ERW (~40 ppm) reported previously (Taylor *et al* 2016). However, those results were based on the hypothetical case of distributing crushed basalt (1 kg m^{-2} yr^{-1}) over a large area of tropical forests (20 million km^2) under RCP4.5 (Taylor *et al* 2016). Co-deployment of both NETs in our simulations doubled the end-of-century CO_2 reduction to 23 ppm (figure 2(a)) indicating their additive effects on net carbon drawdown without adverse carbon cycle interactions.

Global temperature responded to reduced radiative forcing from lowered atmospheric CO_2 concentrations with both ERW and CCS reducing mean global warming by 0.06 °C at peak warming in 2076, and 0.1 °C at 2100 (figure 2(b)). These temperature reductions approximately doubled the probability of meeting the 1.5 °C target from 10% to 19% at peak and from 23% to 42% at 2100, compared to the baseline (figures 2(c) and (d)). Co-deployment of both NETs increased the probability of meeting this target three-fold, from 23% to 67% at 2100 (figure 2(d)). For the 2 °C target, already likely in RCP2.6, deployment of both ERW and CCS resulted in small reductions in the probability of exceeding 2 °C peak warming (non-exceedance probability increased from 91% to 95% at peak) and reduced this risk in 2100 by three-quarters (92%–98%) (figures 2(c) and (d)). Potential reductions in agricultural N_2O emissions by ERW decreased mean global temperature by about 0.01 °C in 2100, indicating the effect is approximately a tenth as important as atmospheric CO_2 reductions.

Global carbon cycle dynamical responses differed between NETs on a century timescale. Over the 21st century, ERW removed atmospheric CO_2 and transferred it to the ocean via the addition of alkalinity (green line, figure 2(e)). The removal is not 1:1 because of ocean CO_2 outgassing offsetting artificial drawdown (Hansen *et al* 2013, Taylor *et al* 2016). With CCS deployment, carbon loss from the atmosphere via its direct injection into permanent geological reservoirs leads to ocean carbon loss via outgassing as surface waters equilibrate with the lower atmospheric CO_2 concentration (blue line, figure 2(e)). End-of-century partitioning between the major global carbon cycle reservoirs illustrates these contrasting responses (figure 2(f)).

We extended these global carbon cycle analyses to assess the long-term fate of CO_2 removed by ERW using 10000 year continuous simulations with fully interactive carbon dynamics in the land, ocean and sediment reservoirs (figure 2(e)). Over multi-millennial (10000 year) timescales, carbon storage in the oceans slowly decreased and storage in the ocean sediments (carbonates) and other

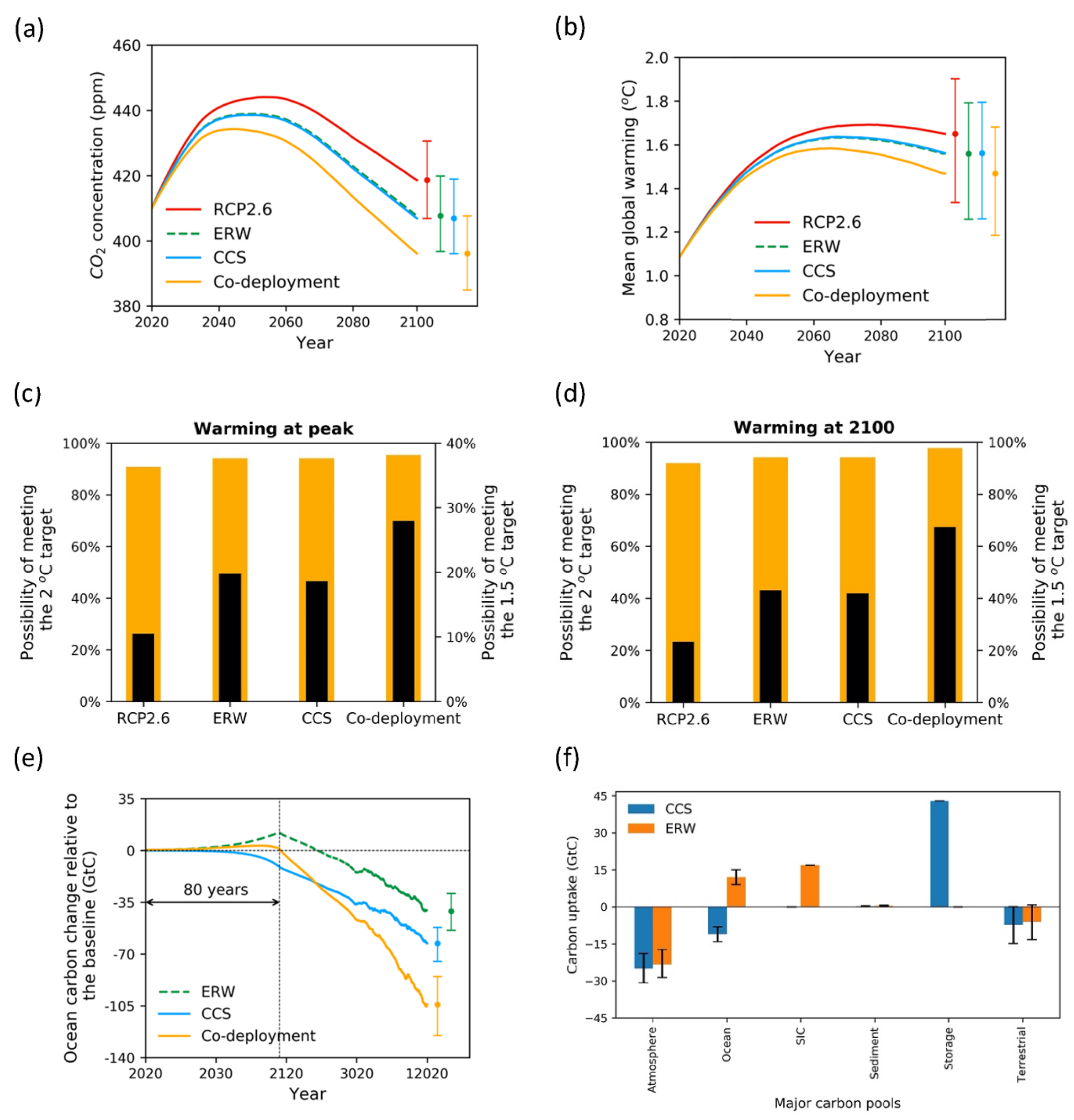

Figure 2. NETs permanently mitigate atmospheric CO_2 concentration and reduce the temperature in RCP2.6 climate change projection (mean values). (a) Atmospheric CO_2 concentration, (b) mean global warming, (c) and (d) the probability of meeting the Paris agreement 1.5° (black) and 2° (orange) warming targets. (e) Variation in the ocean carbon storage relative to the baseline over 10000 years (begins from 2020). Note the logarithmic scale on the *x* axis. (f) Changes in carbon inventories in ERW and CCS scenarios at 2100 with respect to 2020 compared to the baseline (RCP2.6). The 10%–90% confidence interval for each carbon sink is given by an error bar. Note that the values of soil inorganic carbon and storage are calculated directly from the model inputs and do not include uncertainty. In (a), (b) and (e) the 10%–90% confidence interval for each scenario is given by an error bar for the last year, baseline (red), ERW (green), CCS (blue) and co-deployment (orange).

reservoirs increased as the global carbon cycle re-equilibrated (supplementary material figure S2). Differences between three model experiments were maintained consistently over this 10000 year interval (EW, CCS and EW with CCS). Given that carbon is permanently removed from the system in our experimental design in the CCS case, a temporally consistent long-term offset supports carbon removal by ERW as being effectively 'permanent'. These results provide support for prior assumptions regarding the storage security of carbon by removal via ERW derived alkalinity (Renforth and Henderson 2017, The Royal Society and Royal Academy of Engineering 2018) (figure 2(e)).

3.2. The effect of NETs on ocean acidification and marine organisms

Based on the metric of global mean surface ocean pH, both ERW and CCS were equally effective at reducing ocean acidification, increasing it by ~0.01 units by end-of-century relative to the baseline (figure 3(a)). Co-deployment of ERW and CCS doubled this effect mitigating ocean acidification by a global average of 0.02 units, so that by the end of the century, the strategy of co-deployment returned mean ocean pH close to 2020 levels (figure 3(a)).

As expected, the spatial distribution of increased surface ocean pH in ERW and CCS differs (figures 3(b) and (c)). Results for ERW reveal a strong

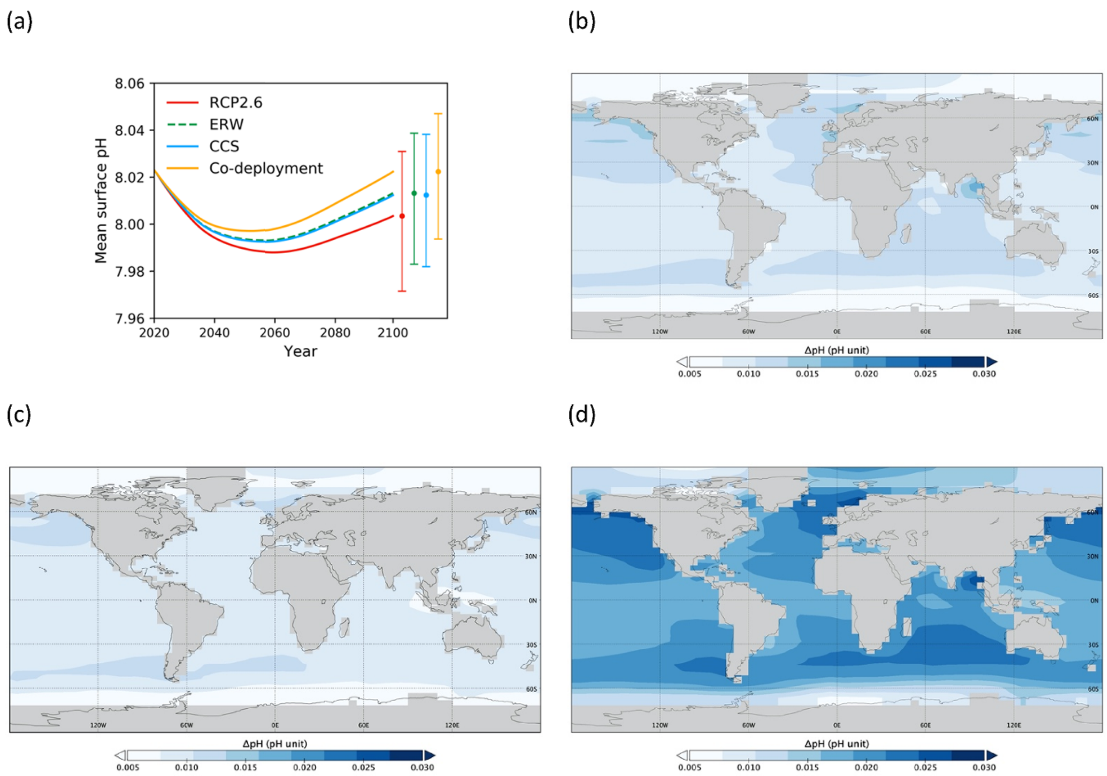

Figure 3. The impact of NETs on the surface ocean pH. (a) Mean surface ocean pH. The 10%–90% confidence interval at 2100 is given by an error bar for each scenario, baseline (RCP2.6) (red), ERW (green), CCS (blue) and co-deployment (orange); (b) the spatial distribution of increased pH in ERW, (c) CCS and (d) co-deployment scenarios relative to the baseline at 2100.

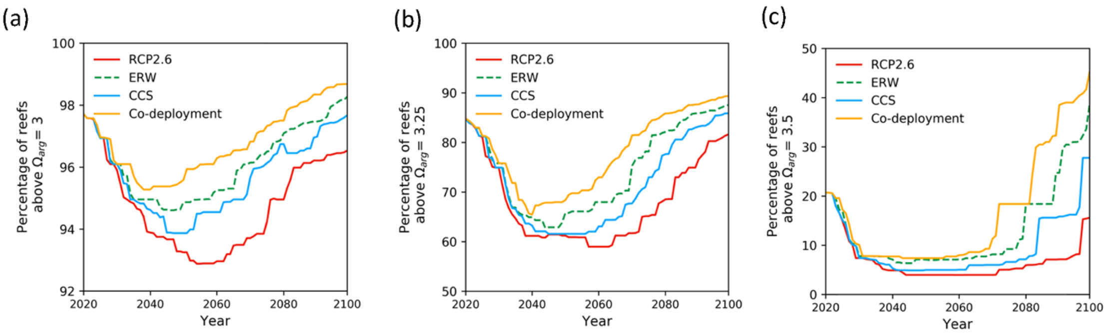

Figure 4. Percentage of coral reefs sites surrounded by global waters with the aragonite saturation state of above (a) 3, (b) 3.25 and (c) 3.5 as a function of time (median values). Note the different scaling of the *y*-axis in each critical aragonite saturation threshold (Ω_{arg}).

signal in south Asia where extensive deployment on croplands produces an alkalinity flux delivered to the surface ocean in the outflows of the major rivers (figure 3(b)). In the CCS scenario, increases in ocean pH are distributed evenly over the ocean surface as a result of global atmospheric CO_2 removal rather than localized delivery of alkalinity (figure 3(c)). Co-deployment of ERW and CCS drives regional increases in surface ocean pH with marked hotpot regions in the Southern Ocean and Eastern Pacific of 0.03 pH units (figure 3(d)). These responses suggest our co-deployment scenario may be sufficient to reverse about one third of the surface ocean acidification effect caused by increases in atmospheric CO_2 since the industrial revolution (0.1 units) (Doney *et al* 2020, Su *et al* 2020).

Coral reefs shift from carbonate accretion towards dissolution where the open ocean Ω_{arg} values fall below a critical threshold due to ocean acidification (Andersson and Gledhill 2013, Fabry *et al* 2008, Gattuso and Hansson 2011, Albright *et al* 2016). We therefore analysed how changes in ocean acidification with NET deployment for atmospheric CO_2 drawdown affected Ω_{arg} in relation to the geographical distribution of coral reefs (figure 4).

In RCP2.6 without additional NET deployment, the percentage of coral reefs above aragonite saturation thresholds of 3, 3.25 and 3.5 decreases from

2020 to 2050, and from that minimum then begins to increase towards the end of the century as atmospheric CO_2 levels decline (figure 4). ERW and CCS deployment increases the percentage of coral reefs above each of the three Ω_{arg} thresholds from 2050 onwards. ERW raised the end-of-century Ω_{arg} state more than CCS in all simulation due to changes in atmospheric CO_2 combined with ERW produced alkalinity flux to the ocean. The magnitude of the protective effects increased with higher Ω_{arg} values. For the highest threshold case (3.5), where the differences between NETs is most marked, we find RCP2.6 leaves 84% of reefs vulnerable to dissolution in 2100 whereas ERW protects ~39% of reefs, CCS ~28% and ERW with CCS ~45%.

4. Discussion

Action on climate change requires atmospheric CO_2 removal with a suite of NETs (IPCC 2018, The Royal Society and Royal Academy of Engineering 2018), while urgently phasing down fossil fuel CO_2 emissions in the near term remains the highest priority for mitigation policies (Hansen *et al* 2017). This necessitates understanding the effectiveness of NETs deployment both individually and when co-deployed with each other. We have addressed this critically important but understudied aspect of climate change science with intermediate complexity Earth system model simulations of ERW and CCS by a NET, such as direct air capture or bioenergy with CCS. Our analyses highlight that for these two NETs there are no adverse interactions, with the effects on CO_2 removal being simply additive. However, we show that co-benefits for calcifying marine organisms are greater for ERW, which is effectively a form of ocean alkalinisation (Bach *et al* 2019).

Deployment of NETs is unlikely to happen without new policy frameworks or specific enabling reforms (Bellamy *et al* 2021). At present, suitable policies are lacking in spite of the need to reach 100–1000 Gt CO_2 levels of drawdown by 2100 (IPCC 2018). The expectation remains that the costs of CDR would ultimately be balanced by compensating income from carbon tax receipts. However, this source is unlikely to be sufficient in the early stages of development in the 2020s (CCC 2020) and from the 2040s will again collapse to the least amenable sectors to decarbonisation, such as aviation and agriculture, as emissions approach net zero, thus again requiring support to avoid high taxation rates. Furthermore, explicit separation of emission reduction and carbon removal targets is likely to be key to avoiding the perception of CDR as mitigation avoidance (Bellamy *et al* 2021). In this context, although the overall costs of CDR, at least in the UK, are within the scale of existing renewables support (CCC 2020), incentivisation policies based on co-benefits offer an attractive option. Importantly, as well as being associated with existing funding streams, policies around co-benefits may reduce delays in deployment. Given farming is heavily subsidised in most countries, this may be the most practical option to support CDR through ERW in the near term at least (Cox and Edwards 2019). In the USA, farmer subsidies for actions enhancing soil carbon storage are already possible, while the European Commission has proposed the use of funds from the common agriculture policy (CAP) to incentivise CDR by farmers via the farm to fork strategy (Schenuit *et al* 2021). Similar proposals have been made in the UK for the Environmental Land Management Scheme planned to replace the CAP (CCC 2020). Co-benefits for fisheries and reef conservation may potentially provide further opportunities to incentivize ERW.

Overall, NET deployment raised the aragonite saturation rate directly by lowering atmospheric CO_2 and indirectly in the case of ERW by addition of alkalinity. However, considerable uncertainty in the aragonite saturation responses to NET deployment exists, as defined by cumulative distribution functions every 20 years beginning from 2020 (supplementary material figures S3–S5). For all scenarios, we find that the percentage of coral reefs in supersaturated waters with respect to Ω_{arg} of 3.25 varied between 10% and 93% in the 1st three time periods (2020–2080) and between 23% and 96% from 2080 to 2100 within 60% confidence interval. For $\Omega_{arg} = 3.5$, these values are within the range 3%–60% for the 1st three periods and from 4% to about 78% for the last period in all scenarios.

These large uncertainties imply that basing policy responses on central estimates of coral reef damage carries a substantial risk of drastically underestimating actually realised damage. Nevertheless, protecting this biodiversity could greatly impact coastal fisheries, cultural services and tourism which together generate annual revenue of around US $42 billion globally (after conversion to 2020 US dollars) (Gattuso and Hansson 2011). Assuming the average total cost of ERW at around US $160 per tonne of CO_2 drawdown (Beerling *et al* 2020), this revenue amounts to more than 13% of the annual total costs, therefore, it provides an important and sustainable financial incentive for long-term application of ERW unaffected by the fluctuation of carbon price as we approach a net-zero emissions future.

Our simulation framework is based on an intermediate complexity Earth system model (GENIE), a class of models with utility in quantifying large-scale feedbacks and uncertainties of atmospheric CO_2 addition and removal on long timescales (centuries to millennia) not readily tractable with high complexity Earth system models (e.g. Taylor *et al* 2016, Jeltsch-Thömmes *et al* 2020). The carbon-cycle responses of this GENIE configuration have previously been shown to be consistent with those of a 15 model intercomparison (Collins *et al* 2013) that included high complexity models such as HadGEM2-ES, with GENIE ensemble responses spanning the multi-model range (Joos *et al* 2013). In addition, the simulated global climate response for RCP2.6 confirms earlier analyses conducted by more complex Earth system models showing it to be broadly consistent with the 2 °C Paris agreement target, and calculated mean end-of-century surface pH (8.0), in agreement with IPCC projections (Bopp *et al* 2013). Thus, the results of our simulations offer a realistic first assessment of ERW and CCS deployment. We recognize however that higher-complexity modelling is required for evaluation of local scale impacts that cannot be reliably resolved at our model resolution.

Here, for simplicity, and in the absence of field data, we neglected modification or precipitation of dissolved inorganic carbon and alkalinity in rivers and estuaries, and assumed the fluxes resulting from ERW are delivered unaltered to coastal ocean cells. However, observation and modelling studies of riverine and coastal mixing processes (Kwon *et al* 2021) suggest a greater delivery of land carbon from rivers and groundwater to the oceans than previously realized. This supports our assumption for efficient delivery of ERW products from rivers to the oceans. In focusing on alkalinity and ocean pH effects, we neglect possible increases in dissolved silica fluxes and trace elements (Beerling *et al* 2018, Bach *et al* 2019) in stream water and ultimately the oceans. Additionally, increased silica delivery might favour diatoms over problematic non-siliceous algae to benefit fisheries production (Sommer *et al* 2002, Ittekkot *et al* 2006) and could strengthen CO_2 removal by stimulation of the oceanic biological pump (Köhler *et al* 2010). The importance of marine nutrient biogeochemistry to microbial activities (Köhler *et al* 2013, Moore *et al* 2013), however, makes further investigation of the extent to which ERW can mitigate the nutrient limitation worthwhile.

Another limitation of the current work is that silicate weathering rates underpinning ERW are sensitive to climate changes, including temperature and soil hydrology, and legacy effects of repeated rock dust applications that allow CDR per unit area to rise over time (Taylor *et al* 2016, Edwards *et al* 2017, Beerling *et al* 2020). By using a fixed CDR for the entire 80 year duration of our simulations (2020–2100), we neglect possible changes in ERW efficiency and consequently CDR associated with both varying climate and repeat ERW treatments (Taylor *et al* 2016). The results of a separate, offline approximation of climate change effects on ERW (section 2.2) suggest a potential 10% error in CDR over 80 years, and highlight the need for further analysis with a detailed dynamic ERW model.

5. Conclusion

In this study, we investigated the possible future behaviour of the Earth system in response to 2 Gt CO_2 yr^{-1} drawdown by ERW deployment on croplands for 80 years within the context of the RCP2.6 mitigation scenario. Our analyses compare CDR via ERW deployment with equivalent CDR via CCS and with co-deployment scenarios of both ERW and CCS. The conclusions below were made accordingly:

- ERW increases the probability of meeting the 1.5 °C Paris target at 2100 from 23% to 42%, while co-deployment increased this further to 67%. The results confirmed that the 2 °C temperature target is likely to be met in RCP2.6. The difference between the 1.5 °C and 2 °C thresholds, however, is likely to be decisive for the survival of many reefs, especially those located in the tropics (Climate Action Tracker 2020).
- The individual ERW and CCS deployment scenarios decreased the atmospheric CO_2 concentration similarly by 11 ppm and reduced global temperature rising to 1.56 °C by the end of the century. Co-deployment of both NETs had additive effects (i.e. 0.1 °C cooling each with ERW and CCS, and 0.2 °C cooling with co-deployment) without adverse Earth system interactions diminishing CO_2 sequestration effectiveness.
- The co-benefit of ERW on ocean chemistry could further improve the living conditions of environmentally sensitive reef-building corals by reducing ocean acidification, especially in south Asia. Nevertheless, the results of all NET deployment scenarios indicate large uncertainties regarding the reversibility of the consequences of high-level climate change mitigation (RCP2.6).

Data availability

The data that supports the findings of this study are available from the corresponding author upon reasonable request.

Acknowledgments

We thank Andy Ridgwell and Steven Banwart for earlier discussions and gratefully acknowledge funding with a Leverhulme Research Centre Award (RC-2015-029) from the Leverhulme Trust.

ORCID iDs

Negar Vakilifard https://orcid.org/0000-0003-1596-1587
Euripides P Kantzas https://orcid.org/0000-0002-7610-1874

Neil R Edwards https://orcid.org/0000-0001-6045-8804
Philip B Holden https://orcid.org/0000-0002-2369-0062
David J Beerling https://orcid.org/0000-0003-1869-4314

References

Albright R *et al* 2016 Reversal of ocean acidification enhances net coral reef calcification *Nature* **531** 362–5

Andersson A J and Gledhill D 2013 Ocean acidification and coral reefs: effects on breakdown, dissolution, and net ecosystem calcification *Annu. Rev. Mar. Sci.* **5** 321–48

Annan J D and Hargreaves J C 2010 Efficient identification of ocean thermodynamics in a physical/biogeochemical ocean model with an iterative Importance Sampling method *Ocean Model.* **32** 205–15

Bach L T, Gill S J, Rickaby R E M, Gore S and Renforth P 2019 CO_2 removal with enhanced weathering and ocean alkalinity enhancement: potential risks and co-benefits for marine pelagic ecosystems *Front. Clim.* **1** 7

Bednar J, Obersteiner M and Wagner F 2019 On the financial viability of negative emissions *Nat. Commun.* **10** 8–11

Beerling D J *et al* 2018 Farming with crops and rocks to address global climate, food and soil security *Nat. Plants* **4** 138–47

Beerling D J *et al* 2020 Potential for large-scale CO_2 removal via enhanced rock weathering with croplands *Nature* **583** 242–8

Bellamy R, Fridahl M, Lezaun J, Palmer J, Rodriguez E, Lefvert A, Hansson A, Grönkvist S and Haikola S 2021 Incentivising bioenergy with carbon capture and storage (BECCS) responsibly: comparing stakeholder policy preferences in the United Kingdom and Sweden *Environ. Sci. Policy* **116** 47–55

Blanc-Betes E, Kantola I B, Gomez-Casanovas N, Hartmann M D, Parton W J, Lewis A L, Beerling D J and DeLucia E H 2021 In silico assessment of the potential of basalt amendments to reduce N_2O emissions from bioenergy crops *Glob. Change Biol. Bioenergy* **13** 224–41 (https://onlinelibrary.wiley.com/journal/17571707)

Board O S and Council N R 2015 *Climate Intervention: Carbon Dioxide Removal and Reliable Sequestration* (Washington, DC: National Academies Press) (https://doi.org/10.17226/18805)

Bopp L *et al* 2013 Multiple stressors of ocean ecosystems in the 21st century: projections with CMIP5 models *Biogeosciences* **10** 6225–45

Brady P V 1991 The effect of silicate weathering on global temperature and atmospheric CO_2 *J. Geophys. Res.* **96** 18101–6

Climate Action Tracker 2020 Scaling up climate action in Australia (available at: https://climateactiontracker.org/documents/806/CAT_2020-11-10_ScalingUp_AUSTRALIA_FullReport.pdf) (accessed 10 May 2021)

Colbourn G, Ridgwell A and Lenton T M 2013 The rock geochemical model (RokGeM) v0.9 *Geosci. Model Dev.* **6** 1543–73

Collins M *et al* 2013 Chapter 12: Long-term climate change: projections, commitments and irreversibility *Climate Change 2013: The Physical Science Basis. Contribution of Working Group I to the fifth Assessment Report of the Intergovernmental Panel on Climate Change* ed T F Stocker *et al* (Cambridge: Cambridge University Press) 1029–136

Committee on Climate Change (CCC) 2020 Policies for the sixth carbon budget and net zero (available at: www.theccc.org.uk/wp-content/uploads/2020/12/Policies-for-the-Sixth-Carbon-Budget-and-Net-Zero.pdf)

Cox E and Edwards N R 2019 Beyond carbon pricing: policy levers for negative emissions technologies *Clim. Policy* **19** 1144–56

Doney S C, Busch D S, Cooley S R and Kroeker K J 2020 The impacts of ocean acidification on marine ecosystems and reliant human communities *Annu. Rev. Environ. Resour.* **45** 83–112

Edwards D P, Lim F, James R H, Pearce C R, Scholes J, Freckleton R P and Beerling D J 2017 Climate change mitigation: potential benefits and pitfalls of enhanced rock weathering in tropical agriculture *Biol. Lett.* **13** 20160715

Edwards N R and Marsh R 2005 Uncertainties due to transport-parameter sensitivity in an efficient 3D ocean-climate model *Clim. Dyn.* **24** 415–33

Fabry V J, Seibel B A, Feely R A and Orr J C 2008 Impacts of ocean acidification on marine fauna and ecosystem processes *ICES J. Mar. Sci.* **65** 414–32

Fekete B M, Vorosmarty C J and Grabs W 2000 Global, composite runoff fields based on observed river discharge and simulated water balances *Tech. Rep.* (Global Runoff Data Center)

Fekete B M, Vörösmarty C J and Grabs W 2002 High-resolution fields of global runoff combining observed river discharge and simulated water balances *Glob. Biogeochem. Cycles* **16** 1042–52

Foley A M, Holden P B, Edwards N R, Mercure J-F, Salas P, Pollitt H and Chewpreecha U 2016 Climate model emulation in an integrated assessment framework: a case study for mitigation policies in the electricity sector *Earth Syst. Dyn.* **7** 119–32

Gattuso J-P and Hansson L 2011 *Ocean Acidification* (Oxford: Oxford University Press)

Guinotte J M, Buddemeier R W and Kleypas J A 2003 Future coral reef habitat marginality: temporal and spatial effects of climate change in the Pacific basin *Coral Reefs* **22** 551–8

Hansen J *et al* 2013 Assessing 'dangerous climate change': required reduction of carbon emissions to protect young people, future generations and nature *PLoS One* **8** e81648

Hansen J *et al* 2017 Young people's burden : requirement of negative CO_2 emissions *Earth Syst. Dyn.* **8** 577–616

Hartmann J, West A J, Renforth P, Köhler P, De La Rocha C L, Wolf-Gladrow D A, Dürr H H and Scheffran J 2013 Enhanced chemical weathering as a geoengineering strategy to reduce atmospheric carbon dioxide, supply nutrients, and mitigate ocean acidification *Rev. Geophys.* **51** 113–49

Holden P B, Edwards N R, Gerten D and Schaphoff S 2013a A model-based constraint on CO_2 fertilisation *Biogeosciences* **10** 339–55

Holden P B, Edwards N R, Müller S A, Oliver K I C, Death R M and Ridgwell A 2013b Controls on the spatial distribution of oceanic $\delta^{13}C_{DIC}$ *Biogeosciences* **10** 1815–33

Honegger M and Reiner D 2018 The political economy of negative emissions technologies: consequences for international policy design *Clim. Policy* **18** 306–21

Intergovernment Panel on Climate Change (IPCC) 2001 *Climate Change 2001: The Scientifc Basis* (Cambridge: Cambridge University Press)

Intergovernment Panel on Climate Change (IPCC) 2018 Global Warming of 1.5 °C. An IPCC Special Report on the Impacts of Global Warming of 1.5 °C above Pre-industrial Levels and Related Global Greenhouse Gas Emission Pathways in *the Context of Strengthening the Global Response to the Threat of Climate Change*

Ittekkot V, Unger D, Humborg C and Tac A N 2006 *The Silicon Cycle: Human Perturbations and Impacts on Aquatic Systems* (Washington, DC: Island Press)

Jeltsch-Thömmes A, Stocker T F and Joos F 2020 Hysteresis of the Earth system under positive and negative CO_2 emissions *Environ. Res. Lett.* **15** 124026

Joos F *et al* 2013 Carbon dioxide and climate impulse response functions for the computation of greenhouse gas metrics: a multi-model analysis *Atmos. Chem. Phys.* **13** 2793–825

Kelland M E *et al* 2020 Increased yield and CO_2 sequestration potential with the C_4 cereal Sorghum bicolor cultivated in basaltic rock dust-amended agricultural soil *Glob. Change Biol.* **26** 3658–76

Kleypas J A, Buddemeier R W, Archer D, Gattuso J-P, Langdon C and Opdyke B N 1999 Geochemical consequences of increased atmospheric carbon dioxide on coral reefs *Science* **284** 118–20

Köhler P, Abrams J F, Völker C, Hauck J and Wolf-Gladrow D A 2013 Geoengineering impact of open ocean dissolution of olivine on atmospheric CO_2, surface ocean pH and marine biology *Environ. Res. Lett.* **8** 014009

Köhler P, Hartmann J and Wolf-Gladrow D A 2010 Geoengineering potential of artificially enhanced silicate weathering of olivine *Proc. Natl Acad. Sci.* **107** 20228–33

Kwon E Y, DeVries T, Galbraith E D, Hwang J, Kim G and Timmermann A 2021 Stable carbon isotopes suggest large terrestrial carbon inputs to the global ocean *Glob. Biogeochem. Cycles* **35** e2020GB006684

Manning D A C and Renforth P 2013 Passive sequestration of atmospheric CO_2 through coupled plant-mineral reactions in urban soils *Environ. Sci. Technol.* **47** 135–41

Millero F J 1995 Thermodynamics of the carbon dioxide system in the oceans *Geochim. Cosmochim. Acta* **59** 661–77

Mollica N R, Guo W, Cohen A L, Huang K-F, Foster G L, Donald H K and Solow A R 2018 Ocean acidification affects coral growth by reducing skeletal density *Proc. Natl Acad. Sci.* **115** 1754–9

Moore C M *et al* 2013 Processes and patterns of oceanic nutrient limitation *Nat. Geosci.* **6** 701–10

New M, Hulme M and Jones P 1999 Representing twentieth century space-time climate variability. Part I: development of a 1961–90 mean monthly terrestrial climatology *J. Clim.* **12** 829–56

Reay D S, Davidson E A, Smith K A, Smith P, Melillo J M, Dentener F and Crutzen P J 2012 Global agriculture and nitrous oxide emissions *Nat. Clim. Change* **2** 410–6

Renforth P and Henderson G 2017 Assessing ocean alkalinity for carbon sequestration *Rev. Geophys.* **55** 636–74

Ricke K L, Orr J C, Schneider K and Caldeira K 2013 Risks to coral reefs from ocean carbonate chemistry changes in recent Earth system model projections *Environ. Res. Lett.* **8** 034003

Ridgwell A J 2001 Glacial-interglacial perturbations in the global carbon cycle PhD Thesis University of East Anglia, Norwich, UK (available at: http://andy.seao2.org/pubs/ridgwell_2001.pdf) (accessed 8 July 2021)

Ridgwell A, Hargreaves J C, Edwards N R, Annan J D, Lenton T M, Marsh R, Yool A and Watson A 2007 Marine geochemical data assimilation in an efficient Earth system model of global biogeochemical cycling *Biogeosciences* **4** 87–104

Ridgwell A and Hargreaves J 2007 Regulation of atmospheric CO_2 by deep-sea sediments in an Earth system model *Glob. Biogeochem. Cycles* **21** GB2008

Schenuit F, Colvin R, Fridahl M, McMullin B, Reisinger A, Sanchez D L, Smith S M, Torvanger A, Wreford A and Geden O 2021 Carbon dioxide removal policy in the making: assessing developments in 9 OECD cases *Front. Clim.* **3** 638805

Sommer U, Stibor H, Katechakis A, Sommer F and Hansen T 2002 Pelagic food web configurations at different levels of nutrient richness and their implications for the ratiofish production: primary production *Hydrobiologia* **484** 11–20

Strefler J, Amann T, Bauer N, Kriegler E and Hartmann J 2018 Potential and costs of carbon dioxide removal by enhanced weathering of rocks *Environ. Res. Lett.* **13** 034010

Su J *et al* 2020 Chesapeake bay acidification buffered by spatially decoupled carbonate mineral cycling *Nat. Geosci.* **13** 441–7

Taylor L L, Quirk J, Thorley R M S, Kharecha P A, Hansen J, Ridgwell A, Lomas M R, Banwart S A and Beerling D J 2016 Enhanced weathering strategies for stabilizing climate and averting ocean acidification *Nat. Clim. Change* **6** 402–6

The Royal Society and Royal Academy of Engineering 2018 Greenhouse gas removal (London)

Tupper M, Tan M K, Tan S L, Radius M J and Abdullah S 2011 ReefBase: a global information system on coral reefs (available at: www.reefbase.org) (accessed 4 May 2020)

van Vuuren D P *et al* 2011 RCP2.6: exploring the possibility to keep global mean temperature increase below 2 °C *Clim. Change* **109** 95–116

West A J, Galy A and Bickle M 2005 Tectonic and climatic controls on silicate weathering *Earth Planet. Sci. Lett.* **235** 211–28

Zeebe R E and Wolf-Gladrow D 2001 *CO_2 in Seawater: Equilibrium, Kinetics, Isotopes (Elsevier Oceanographic Series 65)* (Amsterdam: Elsevier)

Zickfeld K *et al* 2013 Long-term climate change commitment and reversibility: an EMIC intercomparison *J. Clim.* **26** 5782–809